Applied and Environmental Microbiology, Dec. 2010, p. 7972–7980 Vol. 76, No. 24
0099-2240/10/$12.00 doi:10.1128/AEM.01972-10

Inositol Catabolism, a Key Pathway in *Sinorhizobium meliloti* for Competitive Host Nodulation▽†

Petra R. A. Kohler,[1] Jasmine Y. Zheng,[1] Elke Schoffers,[2] and Silvia Rossbach[1]*

Department of Biological Sciences, Western Michigan University, Kalamazoo, Michigan 49008-5410,[1] and Department of Chemistry, Western Michigan University, Kalamazoo, Michigan 49008-5413[2]

Received 19 August 2010/Accepted 18 October 2010

The nitrogen-fixing symbiont of alfalfa, *Sinorhizobium meliloti*, is able to use *myo*-inositol as the sole carbon source. Putative inositol catabolism genes (*iolA* and *iolRCDEB*) have been identified in the *S. meliloti* genome based on their similarities with the *Bacillus subtilis iol* genes. In this study, functional mutational analysis revealed that the *iolA* and *iolCDEB* genes are required for growth not only with the *myo*-isomer but also for growth with *scyllo*- and D-*chiro*-inositol as the sole carbon source. An additional, hypothetical dehydrogenase of the IdhA/MocA/GFO family encoded by the *smc01163* gene was found to be essential for growth with *scyllo*-inositol, whereas the *idhA*-encoded *myo*-inositol dehydrogenase was responsible for the oxidation of D-*chiro*-inositol. The putative regulatory *iolR* gene, located upstream of *iolCDEB*, encodes a repressor of the *iol* genes, negatively regulating the activity of the *myo*- and the *scyllo*-inositol dehydrogenases. Mutants with insertions in the *iolA*, *smc01163*, and individual *iolRCDE* genes could not compete against the wild type in a nodule occupancy assay on alfalfa plants. Thus, a functional inositol catabolic pathway and its proper regulation are important nutritional or signaling factors in the *S. meliloti*-alfalfa symbiosis.

The sugar alcohol inositol, or cyclohexanehexol, occurs in several different stereoisomers, of which the *myo*-form (Fig. 1, compound 1) is the most abundant (1). *myo*-Inositol plays important structural and signaling roles in animal and plant cells (22). In the environment, *myo*-inositol mainly occurs in the phosphorylated form and is involved in the phosphate cycle of terrestrial and freshwater ecosystems (41). The stereoisomers D-*chiro*- and *scyllo*-inositol have recently attracted attention, because they have shown therapeutic potentials for diabetes and Alzheimer's disease, respectively (11, 21). Although there is only limited knowledge about the metabolism of D-*chiro*- and *scyllo*-inositol (25, 50), the catabolism of *myo*-inositol has been studied in a variety of microorganisms, including some members of the *Firmicutes* (17, 46, 51), *Enterobacteriaceae* (4, 19, 40), and *Rhizobiaceae* (16, 29). The *myo*-inositol catabolic pathway and its regulation are best understood in the Gram-positive bacterium *Bacillus subtilis*. The *B. subtilis iol* genes are organized in a divergon comprising *iolABCDEFGHIJ* and *iolRS* (47–49). In the proposed inositol catabolic pathway, the *myo*-inositol dehydrogenase oxidizes *myo*-inositol to its corresponding ketone 2-keto-*myo*-inositol (2KMI), which is then further catabolized by the actions of IolE, -D, -B, -C, -J, and -A (Fig. 1). The inducer of the inositol catabolic pathway in *B. subtilis* is the product of the IolC reaction, 2-deoxy-5-keto-D-gluconic acid 6-phosphate (DKGP; compound 6 in Fig. 1), which antagonizes the binding of the IolR repressor to the *iol* promoter region (51).

Sinorhizobium meliloti, the nitrogen-fixing symbiont of alfalfa, can use *myo*-inositol as the sole carbon source (15). The *idhA*-encoded *myo*-inositol dehydrogenase had been shown to be required for *myo*-inositol catabolism (15), and more recently, an *S. meliloti iolA* mutant was reported that could not grow with *myo*-inositol as the sole carbon source (5). Based on comparisons with *B. subtilis*, a cluster of genes (*iolRCDEB*) was identified in the genome of *S. meliloti* (http://sequence.toulouse.inra.fr/S.meliloti), but their functional role has not been described. Rhizobial inositol metabolism is of special interest because of its link to the catabolism of a group of nutritional mediators in plant-bacteria interactions known as the rhizopines. Rhizopines, produced by several symbiotic *S. meliloti* and *Rhizobium leguminosarum* bv. *viciae* strains, are inositol derivatives, namely, *scyllo*-inosamine and L-3-*O*-methyl-*scyllo*-inosamine (26, 36, 38, 43). The ability to catabolize these inositol derivatives (rhizopines) has been shown to play a role in competition for nodule occupancy (35), but it seems that the ability to catabolize *myo*-inositol itself may also play a role in plant-bacteria interactions. For example, *R. leguminosarum* bv. *viciae iolA* and *iolD* mutants were reported to be strongly impaired in their ability to compete with the wild type during the nodulation process (14), and a *Sinorhizobium fredii idhA* mutant induced nodules with aberrant ultrastructure and showed reduced nitrogen-fixing ability (16). In contrast, an *S. meliloti idhA* mutant was not affected in the ability to nodulate its host plant or to fix nitrogen, but results from competition experiments have not been reported for *S. meliloti* (15). Here, we present a detailed analysis of the *S. meliloti smc01163*, *iolA*, and *iolRCDEB* genes and elucidate their roles in the catabolism of different inositol isomers and in plant-bacteria interactions.

MATERIALS AND METHODS

Microbiological methods. The bacterial strains and plasmids used in this study are listed in Table 1. *Escherichia coli* strains were grown at 37°C in LB medium (37). Antibiotic concentrations for *E. coli* were 50 μg/ml ampicillin (Ap), 30 μg/ml chloramphenicol (Cm), 15 μg/ml gentamicin (Gm), 25 μg/ml kanamycin

* Corresponding author. Mailing address: Department of Biological Sciences, 3923 Wood Hall, Western Michigan University, Kalamazoo, MI 49008-5410. Phone: (269) 387-5868. Fax: (269) 387-5609. E-mail: Silvia.Rossbach@wmich.edu.

† Supplemental material for this article may be found at http://aem.asm.org/.

▽ Published ahead of print on 22 October 2010.

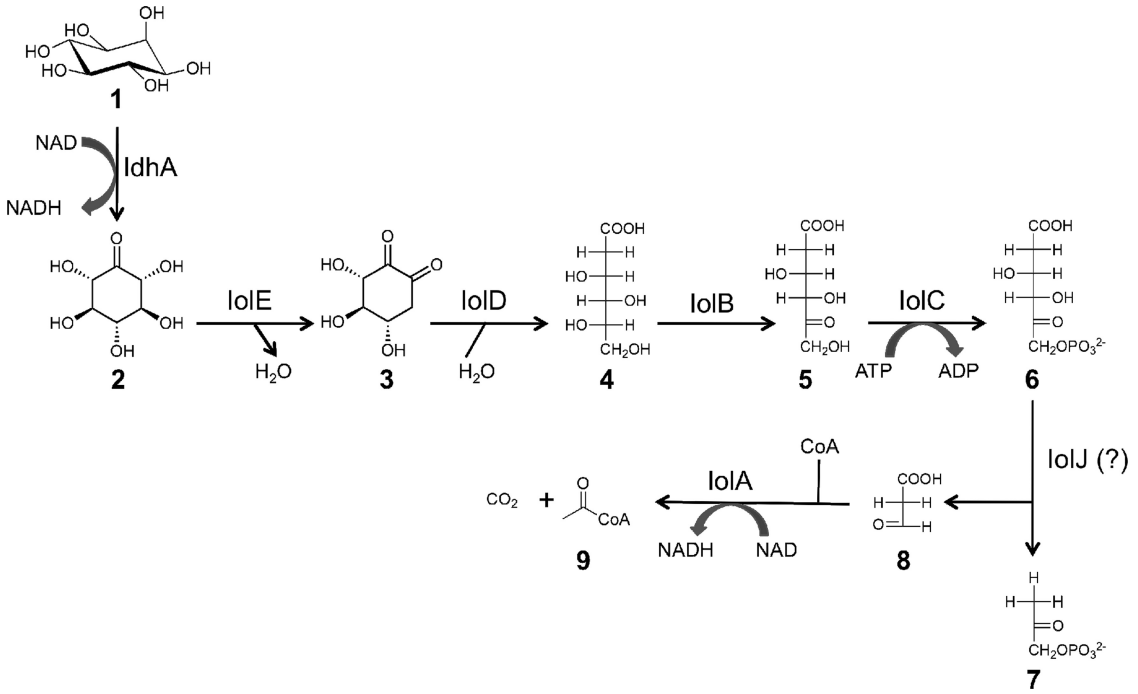

FIG. 1. The proposed *myo*-inositol catabolic pathway (http://www.genome.jp/kegg/). Compound 1, *myo*-inositol (MI); compound 2, 2KMI; compound 3, 3D-(3,4/5) trihydroxycyclohexane-1,2-dione (THcHDO); compound 4, 5-deoxy glucuronic acid (5DG); compound 5, 2-deoxy-5-keto-D-gluconic acid (DKG); compound 6, DKGP; compound 7, dihydroxyacetone phosphate (DHAP); compound 8, malonic semialdehyde (MSA); compound 9, acetyl coenzyme A (acetyl-CoA). Enzymes: IdhA, *myo*-inositol dehydrogenase; IolE, 2KMI dehydratase; IolD, THcHDO hydrolase; IolB, 5DG isomerase; IolC, DKG kinase; IolJ aldolase (not yet identified in *S. meliloti*); IolA, MSA dehydrogenase.

(Km), 25 μg/ml spectinomycin (Sp), and 10 μg/ml tetracycline (Tc). *S. meliloti* cultures were grown at 28°C. Rich media for *S. meliloti* were tryptone yeast (TY) (3) or LB medium supplemented with 2.5 mM $MgSO_4$ and 2.5 mM $CaCl_2$ (LBMC); minimal media were minimal M medium (34) with 0.1% KNO_3 or 0.1% NH_4Cl as sole nitrogen source for the catabolism studies and enzyme assays and GTS minimal medium (18) for the selection of exconjungants. Carbon sources were added to the minimal media at a final concentration of 0.2% unless otherwise indicated. Antibiotic concentrations for *S. meliloti* were 15 μg/ml Gm, 200 μg/ml Km, 250 μg/ml streptomycin (Sm), 200 μg/ml Sp, and 10 μg/ml Tc. For the catabolism studies, *S. meliloti* strains were inoculated 1:100 from TY precultures into liquid minimal M medium. Cultures were grown on a shaking incubator, and the growth was determined spectrophotometrically at 600 nm after 3, 5, and 7 days. Catabolism studies were carried out in duplicate, and values represent the averages of two independent experiments ± the standard errors of the means (SEM).

Preparation of 2-keto-*myo*-inositol. The 2KMI used in this study was synthesized using *Gluconobacter oxydans* (*Acetobacter suboxydans* ATCC 621) according to the methods described by Carter et al. (7) with the following adaptations: *G. oxydans* was grown on sorbitol agar containing 2.5% sorbitol, 0.5% yeast extract, 0.3% peptone, and 1.5% agar or in sorbitol broth containing 10% sorbitol and 0.5% yeast extract. *G. oxydans* was inoculated 1:100 from an overnight preculture into oxidation medium containing 3% *myo*-inositol, 0.5% yeast extract, and 0.1% sorbitol. The oxidation was carried out at 28°C for 4 days. Bacteria were removed from the medium via centrifugation at 6,000 × *g*. The crude product was concentrated and recrystallized from a water-methanol mixture to afford the clean 2KMI.

2-Keto-*myo*-inositol. Melting point 199°C (lit. m.p. 201°C); ^1H NMR (400 MHz, D_2O): δ 4.38 (d, J = 10.2 Hz, 2 H), 3.78 (t, J = 9.5 Hz, 1 H), 3.45 to 3.34 (m, 2 H). The melting point was determined in open capillaries using a Thomas-Hoover Unimelt instrument. The nuclear magnetic resonance (NMR) spectrum was recorded using a 400-MHz Jeol Eclipse nuclear magnetic resonance instrument.

DNA manipulations and microbiological methods. Preparation of plasmid DNA, DNA digests, agarose gel electrophoresis, cloning, and transformation of *E. coli* cells were performed following established protocols (37). Di- and triparental conjugations were performed according to the methods reported by Rossbach and de Bruijn (33).

Construction of *S. meliloti* mutants. Internal DNA fragments of the individual *iolCDEB* genes and a 1,121-bp DNA fragment that contained *smc01163* were PCR amplified from cultures of *S. meliloti* 1021 with the primers listed in Table S1 of the supplemental material. The *iolCDEB* and the *smc01163* PCR products were initially cloned into the pGEM-T or pCR2.1-TOPO vectors (Table 1). The individual *iolCDEB* inserts were recloned into the insertion vector pVO155 (Table 1) and *smc01163* was cloned into the *sacB*-containing suicide vector pJQ200SK (Table 1). An Ω Sm/Sp fragment replaced the 341-bp NruI fragment of *smc01163*, resulting in plasmid pPK63::Ω. The pVO155 vectors carrying the internal fragments of the *iolBCDE* genes and pPK63::Ω were conjugated into *S. meliloti* 1021 with the helper plasmids pRK600 and pRK2013 (Table 1), respectively. The insertion events of the pVO155 derivatives were selected by plating the conjugation mixture onto LBMC Sm Km. The double homologous recombination event with pPK63::Ω was selected for by plating on GTS Sm Sp, followed by counterselection on TY Sm Sp containing 5% sucrose and screening for the absence of the suicide vector on TY Sm Gm. The correct insertions of pVO155 in the individual *iolCDEB* mutants, as well as of the Ω fragment in the *smc01163* deletion mutant, were confirmed by PCR. The transposon (mTn*5*-STM) mutants of *S. meliloti* strain 2011 were provided by Anke Becker (28).

Construction of plasmids for complementation analysis. DNA fragments containing the complete open reading frames (ORFs) of the wild-type *iolC*, *iolD*, *iolE*, and *iolB* genes, including their ribosomal binding sites, were PCR amplified from a liquid *S. meliloti* 2011 culture with primers that were engineered to contain either PstI or NsiI at their 5′ end and BamHI or BglII sites at their 3′ ends (see Table S1 in the supplemental material). The PCR products were cloned into the broad-host-range expression vector pTE3 (Table 1), bringing the PCR products in correct orientation under the control of the *Salmonella trp* promoter, which allows constitutive expression in *S. meliloti* (10). The resulting plasmids carrying the individual *iolCDEB* genes (Table 1) as well as pTE3 as an empty vector control were introduced into the individual *S. meliloti* 1021 and 2011 *iolC*, *iolD*, *iolE*, and *iolB* mutants via triparental mating (33). The presence of the wild-type and of the mutated *iol* genes in the mutant strains was confirmed with PCR.

TABLE 1. Bacterial strains and plasmids used

Strain or plasmid	Relevant characteristics	Reference or source
Escherichia coli strains		
DH5α	*supE44* Δ*lacU169*(ϕ80*lacZ*ΔM15) *hsdR17 recA1 endA1 gyrA96 thi-1 relA1*	37
HB101	*supE44 hsdS20 recA13 ara-14 proA2 lacY1 galK2 rpsL20 xyl-5 mtl-1*	37
Sinorhizobium meliloti strains		
1021	Wild type, Sm^r derivative of SU47	23
2011	Wild type, Sm^r derivative of SU47	24
TIDHA	1021 *idhA*::Tn*5*-56, Sm^r Km^r	15
T63	1021 *smc01163*::Ω, Sm^r Sp^r	This study
TIOLC	1021 *iolC*::pVO155, Sm^r Km^r	This study
TIOLD	1021 *iolD*::pVO155, Sm^r Km^r	This study
TIOLE	1021 *iolE*::pVO155, Sm^r Km^r	This study
TIOLB	1021 *iolB*::pVO155, Sm^r Km^r	This study
WIDHA	2011mTn5STM.5.11.A04, *idhA*::*gus*, Sm^r Km^r	28
W63-1	2011mTn5STM.2.07.F05, *smc01163*::*gus*, Sm^r Km^r	28
W63-2	2011mTn5STM.5.07.B01, *smc01163*::*gus*, Sm^r Km^r	28
WIOLR	2011mTn5STM.4.13.C12, *iolR*::*gus*, Sm^r Km^r	28
WIOLC	2011mTn5STM.1.11.A02, *iolC*::*gus*, Sm^r Km^r	28
WIOLD	2011mTn5STM.1.13.D10, *iolD*::*gus*, Sm^r Km^r	28
WIOLE	2011mTn5STM.1.01.B03, *iolE*::*gus*, Sm^r Km^r	28
WIOLA	2011mTn5STM.4.03.B06, *iolA*::*gus*, Sm^r Km^r	28
WGLYA	2011mTn5STM.4.01.D11, *glyA2*::*gus*, Sm^r Km^r	28
Plasmids		
pVO155	Vector with promoterless *gusA* gene, Ap^r Km^r	27
pJQ200SK	Suicide vector with *sacB* gene, Gm^r	31
pGEM-T	Cloning vector, Ap^r	Promega
pCR2.1-TOPO	Cloning vector, Ap^r Km^r	Invitrogen
pHP45Ω	Source for Ω fragment, Ap^r Sm^r Sp^r	30
pRK2013	*mob tra*, Km^r	12
pRK600	*mob tra*, Cm^r	13
pJZ1	pVO155 containing 301-bp fragment of *iolC*, Km^r	This study
pJZ2	pVO155 containing 270-bp fragment of *iolD*, Km^r	This study
pJZ3	pVO155 containing 226-bp fragment of *iolE*, Km^r	This study
pJZ4	pVO155 containing 399-bp fragment of *iolB*, Km^r	This study
pPK63-1	pJQ200SK containing 1,121-bp fragment of *smc01163*, Gm^r	This study
pPK63Ω	pPK63-1 containing Ω, Gm^r Sm^r Sp^r	This study
pTE3	Broad-host-range expression vector, Tc^r	10
pIOLC	pTE3 containing 2,412-bp fragment of *iolC*	This study
pIOLD	pTE3 containing 2,776-bp fragment of *iolD*	This study
pIOLE	pTE3 containing 945-bp fragment of *iolE*	This study
pIOLB	pTE3 containing 881-bp fragment of *iolB*	This study

β-Glucuronidase assays. The β-glucuronidase assays were optimized based on the methods of Wilson et al. (44). Precultures of *S. meliloti* strains were inoculated 1:100 in 5 ml minimal M medium containing NH_4Cl as N source and either *myo*-inositol, 2KMI, glycerol, glucose, or succinate as C sources. Aliquots (350 μl) of mid-exponential-phase cultures (optical density at 600 nm [OD_{600}], 0.7 to 1) were harvested by centrifugation at 4,500 × *g* for 10 min. The pellet was resuspended in 350 μl GEB buffer (50 mM sodium phosphate buffer [pH 7], 0.6% β-mercaptoethanol, 10 mM EDTA, 1% Triton X-100, 0.1% sodium lauryl sarcosine). After an initial equilibration period of 15 min at 37°C, 35 μl of 20 mM 4-nitrophenyl-β- D-glucuronide (PNPG) was added to the cell lysate. A 100-μl aliquot of the reaction mix was transferred into 800 μl of a 400 mM $NaCO_3$ stop solution after 5, 10, and 15 min. Cell debris was removed by centrifugation at 16,000 × *g* for 30 s, and the OD_{405} was determined spectrophotometrically. The reaction rate was expressed in nmol of *p*-nitrophenol produced per min per OD_{600} unit, ± the SEM. The values represent the means of two independent experiments, and each assay was carried out in duplicate.

NAD(H)-dependent dehydrogenase assays. *S. meliloti* precultures were inoculated 1:100 into 500-ml Erlenmeyer flasks containing 100 ml minimal M medium with NH_4Cl as the N source, glycerol as C source, and either 0.02% *myo*-inositol or 2KMI as inducer. Late-exponential-phase cultures (OD_{600}, 1 to 1.25) were harvested via centrifugation at 6,000 × *g*, washed with 40 mM HEPES buffer (pH 7) containing 10 mM β-mercaptoethanol, and resuspended in 5 ml 40 mM HEPES buffer (pH 7). Cell extracts were prepared with a sonicator at 50 W with three 30-s sonication periods (Misonix XL-2020 [Farmingdale, NY]). The *myo*-, *scyllo*-, and D-*chiro*-inositol dehydrogenase activities were determined at room temperature (21 to 23°C). Each reaction mix (1 ml) contained 50 mM NH_4Cl, 50 mM Na_2CO_3, 100 μl cell extract, and 0.4 mM NAD^+. A baseline of background reduction of NAD^+ in the absence of substrate was established at a wavelength of 340 nm for slope correction. The increase in absorbance (A_{340}) in the presence 25 mM *myo*-, *scyllo*-, or D-*chiro*-inositol was monitored for 3 min. The protein content of the cell extracts was determined with a Bradford assay (Pierce Coomassie Plus: the Better Bradford assay kit; Thermo Fisher Scientific, Rockford, IL). The specific *myo*-, *scyllo*-, and D-*chiro*-inositol dehydrogenase activities are expressed as nmol NAD^+ reduced min^{-1} mg of $protein^{-1}$, ± the SEM. The values represent the means of two independent experiments, each of them performed in duplicate, unless otherwise indicated.

Competition assay for nodule occupancy. Axenic alfalfa (*Medicago sativa*) plants were prepared by germination from surface-sterilized seeds on folded Whatman filter paper in 20 ml of nitrogen-free B&D growth medium (6) in 25-mm-diameter tubes as described previously (36). Plants were grown at room temperature under a cycle of 16 h of light and 8 h of dark. Before inoculation, rhizobial cultures were pelleted, washed, and resuspended in sterile deionized H_2O, and their optical density at 600 nm was determined spectrophotometrically. Mixed cultures of the *S. meliloti* 2011 wild-type and individual mutant strains were prepared in a 1:1 ratio based on the OD_{600} values. In addition, the 1:1 input ratio was verified via serial dilution and plating on TY Sm and TY Sm Km.

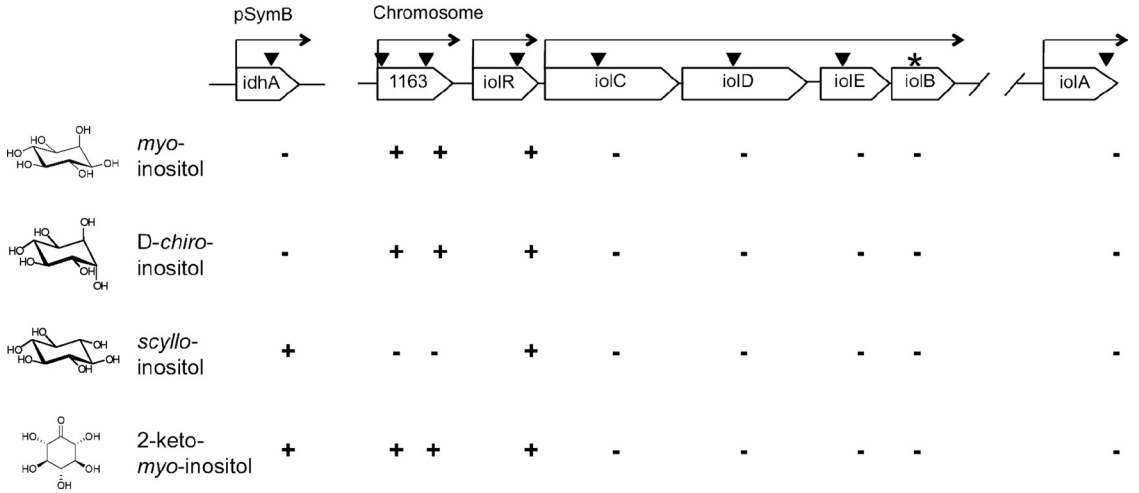

FIG. 2. Ability of *S. meliloti* wild-type and the *idhA*, *smc01163* (1163), *iolR*, *iolC*, *iolD*, *iolE*, *iolA*, and *iolB* mutant strains to grow with 0.2% *myo*-inositol, D-*chiro*-inositol, *scyllo*-inositol, or 2KMI as the sole carbon source in minimal medium. Open reading frames are depicted as open arrows. The locations of the mini-Tn*5* insertions in the *S. meliloti* 2011 mutants are marked by vertical arrowheads. The star indicates the position of the plasmid insertion in the *S. meliloti iolB* mutant. Horizontal arrows above the genes indicate predicted transcriptional units. Each mutant's ability (+) or inability (−) to use inositol compounds as the sole carbon source is indicated.

Seven-day-old alfalfa seedlings were inoculated with 1 ml of the mixed cultures or 1 ml of the wild-type or the individual mutant strains. One milliliter of sterile deionized H_2O was added to control plants. The total number of nodules per plant was determined, and after 20 weeks, the nodules were harvested and surface sterilized with 70% ethanol. Plant fresh and dry weights were determined and averaged from six plants of each treatment group. Rhizobia were reisolated by homogenizing the nodules in sterile H_2O, and serial dilutions were prepared. The wild-type versus the mutant strain output ratio was determined by selective plating on TY Sm and TY Sm Km. The values represent the averages of two independent studies ± the SEM, with six plants each.

RESULTS

Structure and organization of the inositol catabolism genes in *S. meliloti*. In contrast to the organization of the *iol* genes in *B. subtilis*, the inositol catabolism genes of *S. meliloti* are not arranged in a single gene cluster. The *idhA* gene is located on the pSymB plasmid, whereas the putative *iolR*, *iolC*, *iolD*, *iolE*, and *iolB* genes are organized in one cluster on the chromosome, all oriented in the same direction (Fig. 2). The *iolA* gene is located a further 400 kb away on the chromosome. An additional gene of interest, *smc01163*, encoding a putative dehydrogenase of the IdhA/MocA/GFO family, is located directly upstream of *iolR* (Fig. 2). The *S. meliloti* transcriptional regulator encoded by *iolR* belongs to the RpiR repressor family and is a homologue of the IolR regulator in *Caulobacter crescentus* (5). The *iolCDEB* genes are predicted to comprise an operon, whereas the *smc01163* and *iolR* genes seem to be transcribed separately (www.microbesonline.org) (Fig. 2).

Catabolism studies. To conduct a complete study of the roles of the predicted *iol* genes in the catabolism of different inositol stereoisomers, mutants of *S. meliloti* strain 2011 were obtained that contained mTn*5*-STM transposon insertions in the *idhA*, *iolA*, and the individual *iolRCDE* genes, as well as two mutant strains with different insertions in the *smc01163* gene (28). As part of a comparative analysis, mutants were also constructed in the *S. meliloti* 1021 strain, specifically, insertions in *smc01163* and the individual *iolCDEB* genes. The 1021 and 2011 strains are both streptomycin-resistant derivatives of *S. meliloti* SU47 wild type (23, 24), but years of culturing in different laboratories have resulted in minor differences between these two strains (20, 42).

When grown in minimal medium with *myo*-inositol as the sole C source, both wild-type strains grew to an OD_{600} of around 1.2, while their corresponding *idhA*, *iolC*, *iolD*, *iolE*, *iolB*, and *iolA* mutants did not grow (Fig. 2; see also Fig. S2A in the supplemental material). The *iolR* and the three different *smc01163* mutants grew to similar optical densities as the wild type (shown for W63-1 and W63-2 in Fig. 2; also shown for W63-1 in Fig. S2A). In a control experiment, all strains were able to grow with glucose as the sole C source (data not shown). Hence, the *idhA*, *iolA*, and *iolCDEB* genes are essential for *myo*-inositol catabolism in *S. meliloti*. Since the *iolCDEB* genes are predicted to form an operon, the mTn*5*-STM transposon and the plasmid insertions in the *iolC*, *iolD*, and *iolE* genes could have polar effects. We cloned the individual *iolCDEB* genes under the control of a constitutive promoter in the broad-host-range expression vector pTE3 (Table 1). The resulting plasmids were conjugated into the respective *S. meliloti* 1021 *iolC*, *iolD*, *iolE*, and *iolB* mutants as well as into the strain 2011 *iolC*, *iolD*, and *iolE* mutants. The mutant strains containing the plasmids with the individual *iolC*, *iolD*, *iolE*, and *iolB* genes were able to grow with *myo*-inositol as the sole C source, whereas the same strains carrying the empty vector as control could not (see Fig. S3 in the supplemental material). The growth of the mutant strains containing the plasmid with the *iolC*, *iolD*, and *iolE* genes was delayed compared to the wild types or the *iolB* mutant strain containing the *iolB*-carrying plasmid (see Fig. S3). Thus, we conclude that the mTn*5*-STM transposon and the plasmid insertions seem to allow a low level of expression of the downstream *iol* genes, probably due to a weak read-through from the integrated kanamycin resistance genes.

We investigated which other inositol isomers can be catab-

olized by *S. meliloti*. Strains 1021 and 2011 were grown with commercially available *scyllo*-, *muco*-, *allo*-, D-*chiro*-, and L-*chiro*-inositol as sole C source (see Fig. S1 in the supplemental material). Both wild-type strains could grow with *scyllo*- or D-*chiro*-inositol (shown for strain 2011 in Fig. S2B and C in the supplemental material), but they were not able to use L-*chiro*-, *muco*-, or *allo*-inositol (data not shown). The roles of the *iol* genes in the catabolism of *scyllo*- and D-*chiro*-inositol were further investigated. The *idhA* and the *iolR* mutants could grow with *scyllo*-inositol, but the *iolC*, *iolD*, *iolE*, *iolB*, and *iolA* mutants could not (Fig. 2; see also Fig. S2B). Interestingly, all three *smc01163* mutants were unable to grow with *scyllo*-inositol as the sole C source (see Fig. S2B, W63-1). Thus, the *smc01163* gene product appears to be essential for the catabolism of *scyllo*-inositol. D-*chiro*-Inositol was used as the sole C source by the *iolR* and the *smc01163* mutants but not by the *idhA*, *iolC*, *iolD*, *iolE*, *iolB*, and *iolA* mutants (Fig. 2; see also Fig. S2C), suggesting that the *idhA*-encoded *myo*-inositol dehydrogenase facilitates the oxidation of both *myo*- and D-*chiro*-inositol.

We also tested the first proposed intermediate in the *myo*-inositol catabolic pathway, 2KMI, which was synthesized in our laboratory (see Materials and Methods). The *iolC*, *iolD*, *iolE*, *iolB*, and *iolA* mutants did not catabolize 2KMI, but the *idhA*, *iolR*, and *smc01163* mutants could (Fig. 2; see also Fig. S2D). The fact that the *idhA* mutant grew on 2KMI as the sole C source while the *iolA* and *iolCDEB* mutants failed to do so strongly supports the notion that, also in *S. meliloti*, 2KMI is the product of the *myo*-inositol dehydrogenase (IdhA) reaction.

Regulation of *S. meliloti* inositol catabolism. The 2011 *idhA*, *smc01163*, *iolR*, *iolD*, and *iolE* mutants contain the mTn*5*-STM::*gusA* transposon in the same orientation as the respective genes, creating a transcriptional fusion and therefore allowing us to investigate the regulation of the inositol genes by measuring the β-glucuronidase activity (28). Mutant strains were grown in minimal medium with either *myo*-inositol, 2KMI, glycerol, glucose, or succinate as carbon source, or in combinations, to analyze the effects of different carbon sources. Cells were harvested and solubilized, and their β-glucuronidase activities were determined. The wild-type strain, which does not contain a *gusA* gene, served as a negative control and did not exhibit any detectable β-glucuronidase activity (data not shown). The expression of the *idhA* gene in its corresponding mutant was not inducible by *myo*-inositol but was induced in the presence of 2KMI with all carbon sources tested (Fig. 3A). This finding indicates that not *myo*-inositol itself but either 2KMI or a later pathway intermediate functions as an inducer in *S. meliloti*, as has been shown for *B. subtilis* (51). The expression of *smc01163* in its corresponding mutant was induced by *myo*-inositol or 2KMI with all carbon sources tested (Fig. 3B). We did not notice any major catabolite repression effect when glycerol, glucose, or succinate was present in the medium (Fig. 3A and B). The *iolR* gene, encoding the RpiR-like repressor, was constitutively expressed in its corresponding mutant, since high β-glucuronidase activities were displayed under all growth conditions, even for growth without inducer (Fig. 3C). It is interesting that only very low β-glucuronidase activities were observed in the *iolD* and *iolE* mutants in the presence or absence of the inducers *myo*-inositol or 2KMI (between 2 and 3 nmol min^{-1} OD_{600} $unit^{-1}$). This further supports the notion that neither *myo*-inositol nor 2KMI, but a later pathway intermediate which

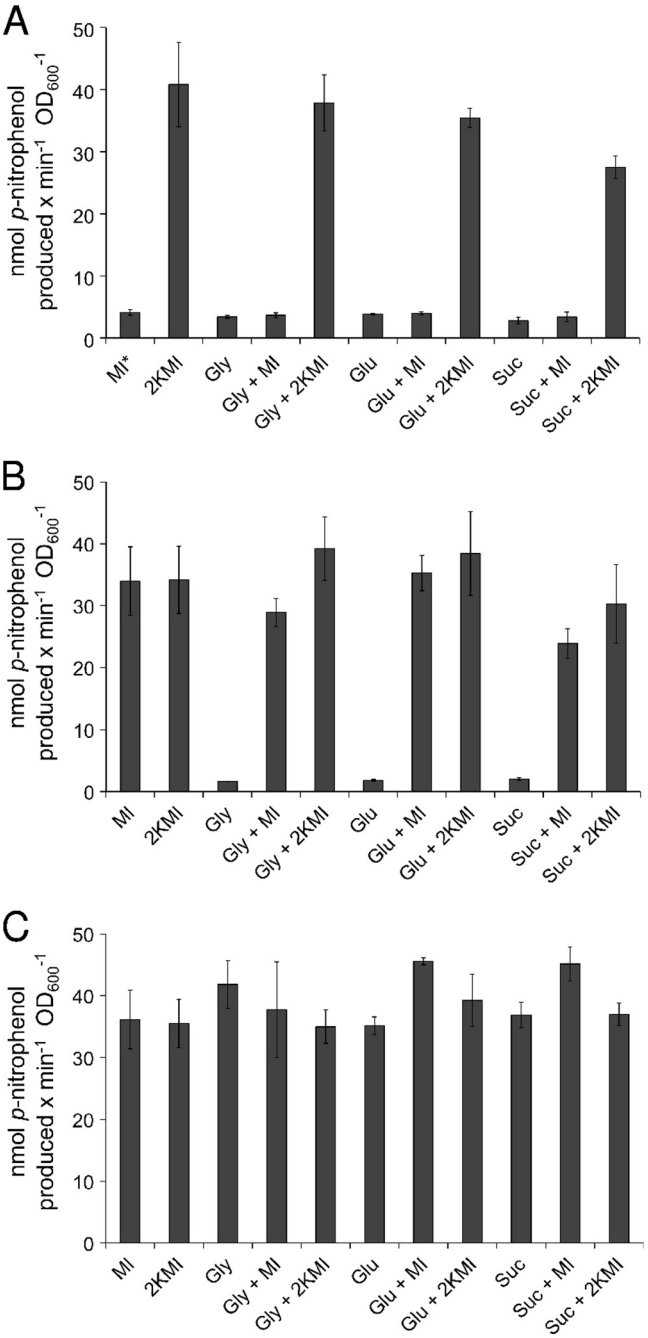

FIG. 3. β-Glucuronidase activities of the *S. meliloti idhA* (A), *smc01163* (B), and *iolR* (C) *gusA* reporter gene fusions in the respective mutant strains. The reaction rate is expressed in nmol *p*-nitrophenol produced per minute per OD_{600} unit. Cultures were grown in minimal medium containing 0.2% of the following carbon sources: *myo*-inositol (MI), 2KMI, glycerol (Gly), glucose (Glu), succinate (Suc), or combinations thereof. Bars represent the averages of two independent experiments, and error bars denote SEM. MI* indicates that the *idhA* mutant did not grow with *myo*-inositol as the sole carbon source in minimal medium, but the residual β-glucuronidase activity is probably due to the carryover of cells from the TY preculture.

TABLE 2. Specific *myo*-inositol dehydrogenase activities of *S. meliloti* wild-type and mutant strains

Strain	Relevant genotype	*myo*-Inositol dehydrogenase sp act (nmol/min/mg of protein)		
		Uninduced	2KMI induced	*myo*-Inositol induced
2011	Wild type	5 ± 0.3	65 ± 9	103 ± 4
1021	Wild type	21 ± 4	79 ± 10	131 ± 7
WIDHA	*idhA*	2 ± 0.3	0.6 ± 0.3	0.5 ± 0
W63-1	*smc01163*	10 ± 4	55 ± 5	103 ± 42
WIOLR	*iolR*	522 ± 2	337 ± 6	410 ± 24
WIOLC	*iolC*	0.2 ± 0.1	0.4 ± 0.1	8 ± 0
WIOLD	*iolD*	2 ± 2	5 ± 1	5 ± 0
WIOLE	*iolE*	0.4 ± 0.2	0 ± 0	5 ± 0
TIOLB	*iolB*	5 ± 1	2 ± 0.3	0.4 ± 0.2

TABLE 3. Specific *scyllo*-inositol dehydrogenase activities of *S. meliloti* wild-type and mutant strains

Strain	Relevant genotype	*scyllo*-Inositol dehydrogenase sp act (nmol/min/mg of protein)	
		2KMI induced	*myo*-Inositol induced
2011	Wild type	74 ± 2	69 ± 1
1021	Wild type	ND[a]	91 ± 2
WIOLR	*iolR*	ND	477[b]
W63-1	*smc01163*	50 ± 5	40 ± 1
W63-2	*smc01163*	39[b]	52[b]
T63	*smc01163*	ND	62 ± 1
WIOLE	*iolE*	ND	3 ± 0.5

[a] ND, not done.
[b] Value is based on one experiment.

cannot be synthesized by the *iolD* or *iolE* mutant, serves as the true inducer in *S. meliloti*.

Determination of *myo*-inositol dehydrogenase activity. For the determination of the *myo*-inositol dehydrogenase activity, an NAD(H)-dependent dehydrogenase assay was used. Cultures were grown in minimal medium containing glycerol as C source and with either *myo*-inositol or 2KMI as inducer. The specific *myo*-inositol dehydrogenase activities of the wild types, the *idhA*, the *smc01163*, and the individual *iolCDEB* mutant strains were low without prior induction (0.2 to 21 nmol min^{-1} mg of $protein^{-1}$) (Table 2). Upon induction with *myo*-inositol, the 2011 and 1021 wild types displayed *myo*-inositol dehydrogenase activities of 103 and 131 nmol min^{-1} mg of $protein^{-1}$, respectively (Table 2). When grown with 2KMI as inducer, the wild-type cells exhibited ~30% lower *myo*-inositol dehydrogenase activities (Table 2). Regardless of whether the *idhA* mutant was induced with *myo*-inositol or 2KMI, its *myo*-inositol dehydrogenase activity was basically abolished (Table 2), which confirmed the results of Galbraith et al. (15), who found that the *idhA* gene, located on the pSymB plasmid, encodes the *myo*-inositol dehydrogenase. All three mutants with insertions in *smc01163* exhibited *myo*-inositol dehydrogenase activities comparable to the wild type (Table 2, W63-1). The *iolR* mutant displayed a 4- to 5-fold-higher *myo*-inositol dehydrogenase activity than the wild type, even when not induced (Table 2). The *iolC*, *iolD*, *iolE*, and *iolB* mutants, however, exhibited very low *myo*-inositol dehydrogenase activities (Table 2), regardless of whether they were grown with or without *myo*-inositol or 2KMI as inducers, indicating that all four gene products (IolC, IolD, IolE, and IolB) are needed for inducer production.

Determination of *scyllo*-inositol dehydrogenase activity. The results of the catabolism studies suggest that the dehydrogenase encoded by *smc01163* functions as a *scyllo*-inositol dehydrogenase. Thus, the *scyllo*-inositol dehydrogenase activities of the wild type and the *smc01163* mutants were investigated. Based on our findings that the *smc01163* gene was inducible by *myo*-inositol and 2KMI (see above), wild-type and mutant strains were grown in minimal medium with glycerol as C source and with *myo*-inositol or 2KMI as inducer. The specific *scyllo*-inositol dehydrogenase activities of the uninduced wild type and the *smc01163* mutants were very low (10 and 5 nmol min^{-1} mg of $protein^{-1}$, respectively). Upon induction with *myo*-inositol, the 2011 and 1021 wild types displayed *scyllo*-inositol dehydrogenase activities of 69 and 91 nmol min^{-1} mg of $protein^{-1}$, respectively, while the three *smc01163* mutants showed between 58% and 75% of the wild-type *scyllo*-inositol dehydrogenase activity (Table 3). The results of the *scyllo*-inositol dehydrogenase assay were unexpected. The *smc01163* mutants were unable to use *scyllo*-inositol as sole C source, suggesting that the *smc01163* gene encodes the *scyllo*-inositol dehydrogenase and the mutants would not exhibit any *scyllo*-inositol dehydrogenase activity. Nevertheless, we obtained the same results for all three *smc01163* mutants, which were constructed independently in two different genetic backgrounds. The *scyllo*-inositol dehydrogenase activities of the *iolR* and *iolE* mutants were also determined. The *iolR* mutant displayed an almost-7-fold-higher *scyllo*-inositol dehydrogenase activity than the wild type (Table 3). The *scyllo*-inositol dehydrogenase activity of the *iolE* mutant was very low (Table 3). When the *scyllo*-inositol dehydrogenase activity was determined from cultures grown with 2KMI as inducer, similar results were obtained (Table 3).

Determination of D-*chiro*-inositol dehydrogenase activity. The 2011 wild type and the corresponding *idhA* and *iolR* mutants were subjected to a D-*chiro*-inositol dehydrogenase assay. The wild type displayed a D-*chiro*-inositol dehydrogenase activity of 52 ± 0.2 nmol min^{-1} mg of $protein^{-1}$, while the *idhA* mutant showed only marginal dehydrogenase activity in the presence of D-*chiro*-inositol (0.3 ± 0.1 nmol min^{-1} mg of $protein^{-1}$). The D-*chiro*-inositol dehydrogenase activity of the WIOLR mutant was increased 4-fold (235 ± 10 nmol min^{-1} mg of $protein^{-1}$).

Competition assay for nodule occupancy. To investigate the role of *S. meliloti* inositol catabolism during symbiotic interactions, a competition assay for nodule occupancy was performed with the 2011 wild type and each of the *idhA*, *smc01163*, *iolR*, *iolC*, *iolD*, *iolE*, and *iolA* mutants. The wild type and the individual mutant strains were inoculated onto axenic alfalfa plants in a 1:1 ratio and as single inoculants as controls. All strains nodulated the host plants successfully when inoculated individually. Plants developed six nodules on average, and there was no difference between the average fresh and dry weight of the plants nodulated by the wild type (average fresh weight, 131 ± 12 g; average dry weight, 14 ± 2 g) or by the individual mutant strains (average fresh weight, 138 ± 16 g; average dry weight, 14 ± 2 g). Twenty weeks postinoculation, the nodules

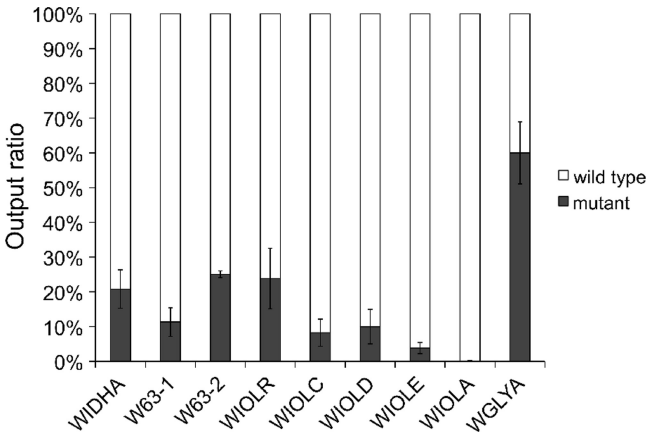

FIG. 4. Competition assay for nodule occupancy. The *S. meliloti* 2011 *idhA* (WIDHA), *smc01163* (W63-1 and W63-2), *iolR* (WIOLR), *iolC* (WIOLC), *iolD* (WIOLD), *iolE* (WIOLE), *iolA* (WIOLA), and *glyA2* (WGLYA) mutant strains were inoculated on alfalfa plants in a 1:1 ratio with the wild type. After 20 weeks nodules were harvested and surface sterilized, and rhizobia were reisolated from the nodules. The wild-type versus the mutant output ratio of the reisolated rhizobia was determined via selective plating. Bars represent the averages of two independent experiments representing nodules from six plants each. Error bars denote SEM.

were harvested and rhizobia were reisolated from surface-sterilized nodules. On average, 10^6 bacteria were reisolated from the nodules of one plant, and the output ratio of kanamycin-resistant (mutant) to kanamycin-sensitive rhizobia (wild type) was determined by selective plating. If a gene does not play a role in the competition for nodule occupancy, the same output as input ratio (50:50) is expected. This was true for a control mutant (WGLYA) that carried an mTn*5*-STM insertion in an unrelated gene, since WGLYA was reisolated from the nodules with a frequency of 60%, which was similar to the input ratio of 50% (Fig. 4). In contrast, the mutants with insertions in the *idhA*, *smc01163*, *iolR*, *iolC*, *iolD*, *iolE*, or *iolA* genes represented only a small fraction of the rhizobia reisolated from the nodules. The values varied between 0.15% for the *iolA* mutant and 25% for the *smc01163* mutant (Fig. 4). Thus, the *idhA*, *smc01163*, and *iol* mutants were outcompeted by the wild type in all cases, showing that a functional inositol catabolic pathway, the transcriptional regulator IolR, and the dehydrogenase encoded by *smc01163* are all required for successful competition during alfalfa nodulation. We also determined the wild type/mutant output ratios after 10 and 15 weeks, with essentially the same results (data not shown).

DISCUSSION

We have shown that the *iolA* and *iolCDEB* genes are essential not only for *myo*-inositol but also for *scyllo*- and D-*chiro*-inositol catabolism in *S. meliloti*. It is interesting that *myo*- and especially *scyllo*-inositol serve as excellent carbon sources for *S. meliloti*, since the wild types grew to an OD_{600} of >1 in minimal medium, which is comparable to growth with other C sources, such as glucose, glycerol, or succinate. This is in contrast to *B. subtilis*, which does not grow as efficiently with *myo*- or *scyllo*-inositol as with glucose (25). Similarly, a lag time of 60 h has been reported for *Salmonella enterica* when grown with *myo*-inositol (19).

The *idhA*-encoded *myo*-inositol dehydrogenase acts on *myo*- and D-*chiro*-inositol. The *idhA* mutant could not grow with *myo*- or with D-*chiro*-inositol as the sole C source. As confirmation, cell extracts of the *idhA* mutant did not display any detectable dehydrogenase activity when *myo*- or D-*chiro*-inositol was offered as substrate in the enzyme assay. Thus, we conclude that the initial dehydrogenation of *myo*- as well as of D-*chiro*-inositol is carried out by the *idhA*-encoded dehydrogenase. This is not without precedent; the purified *myo*-inositol dehydrogenase of *B. subtilis* has been shown to oxidize both *myo*- and D-*chiro*-inositol (8). The *S. meliloti idhA* mutant was able to use *scyllo*-inositol as the sole C source, indicating that there is at least one other dehydrogenase involved in the oxidation of *scyllo*-inositol and that *scyllo*-inositol is probably not a substrate for the *myo*-inositol dehydrogenase. In fact, *scyllo*-inositol could not react with the purified *myo*-inositol dehydrogenase of *B. subtilis* (32), and our preliminary data revealed that *scyllo*-inositol is not a substrate for the *idhA* gene product overexpresssed in *E. coli* (P. R. A. Kohler, unpublished observation).

Inositol catabolism in *S. meliloti* requires induction through a pathway intermediate. The results from the β-glucuronidase and NAD(H)-dependent dehydrogenase assays clearly demonstrated that functional *idhA*, *iolC*, *iolD*, *iolE*, and *iolB* genes are required for induction of the *iol* genes. Thus, the inositol catabolism genes are not necessarily induced by inositol but by a later pathway intermediate. This is comparable to *B. subtilis*, in which the binding of DKGP to the negative regulator IolR antagonizes the transcriptional repression of the *iol* genes (51). DKGP is the fifth intermediate in the pathway and the product of the IolC reaction (Fig. 1). Usually, *myo*-, *scyllo*-, and D-*chiro*-inositol occur together in soil (41), and that may explain the advantage a common pathway intermediate would offer as an inducer over a specific inositol isomer.

IolR negatively regulates the activities of the *myo*- and *scyllo*-inositol dehydrogenases. The *iolR* mutant was able to grow with *myo*-, *scyllo*-, and D-*chiro*-inositol and 2KMI as sole C sources, demonstrating that the *iolR* gene is not a structural gene in the inositol catabolic pathway. Nevertheless, the *iolR* gene is required for the regulation of the *myo*- and *scyllo*-dehydrogenase activities in *S. meliloti*, since the activity of both enzymes was 4- to 7-fold higher in the *iolR* mutant than in the wild type (Tables 2 and 3). The *S. meliloti* IolR, like IolR from *C. crescentus*, belongs to the RpiR repressor family (5). In *C. crescentus*, a conserved DNA sequence, GGAANATNCGTTCCA, was identified in the promoter region of the *iol* genes as a probable IolR-binding site (5). Computational predictions revealed related motifs in *S. meliloti* upstream of the *idhA*, *iolR*, and *iolC* genes (5). Interestingly, we detected a similar sequence ~80 bp upstream of the start codon of *smc01163* (CGAATAAATATTCCA). Our biological data confirm that IolR represses the *myo*- and *scyllo*-inositol dehydrogenase activities. The presence of a putative IolR-binding site upstream of *iolR* and the constitutive expression of the *iolR-gusA* fusion in the *iolR* mutant indicate that IolR negatively regulates its own expression.

The *smc01163* gene is essential for *scyllo*-inositol metabolism. None of the three different *smc01163* mutants con-

structed in two different strains was able to grow with *scyllo*-inositol as the sole C source. Thus, the putative dehydrogenase encoded by the *smc01163* gene is essential for *scyllo*-inositol catabolism. Nevertheless, the *smc01163* mutants displayed 58 to 75% of the wild-type dehydrogenase activity when *scyllo*-inositol was offered as the substrate in the enzyme assay. We can exclude nonspecific NAD^+ reduction through background activity, because the background NAD^+-reducing activity was determined for each cell extract in the absence of the substrate for slope correction. All strains showed little NAD^+-reducing background activities (1 to 5% of the *myo*- and *scyllo*-inositol dehydrogenase activities). In addition, we determined the enzyme activities in the presence of various substrate concentrations to ensure substrate specificity (data not shown).

Although *smc01163* encodes a dehydrogenase essential for *scyllo*-inositol catabolism, this enzyme may not be the only dehydrogenase that interacts with *scyllo*-inositol. Recently, two *scyllo*-inositol dehydrogenases were identified in *B. subtilis*, IolX and IolW (25). Both purified enzymes reacted with *scyllo*-inositol, but only the *iolX* mutant showed impaired growth with *scyllo*-inositol as the sole C source (25). Interestingly, our computational analysis of the *smc01163*-deduced protein predicts the presence of an N-terminal signal peptide. Thus, a periplasmic location of SMc01163 is probable. We conclude that the catabolism of *scyllo*-inositol in *S. meliloti* may require at least one additional, probably cytoplasmic enzyme. This might explain the results of the growth studies compared to the results from the *scyllo*-dehydrogenase assays using crude cell extracts. SMc01163 seems to be essential for the initial interaction with *scyllo*-inositol in the periplasm, but this reaction is bypassed when the cell is lysed by sonication for the dehydrogenase assay. Another enzyme, not the one encoded by *smc01163*, oxidizes *scyllo*-inositol in the cytoplasm of *S. meliloti* and was detectable as *scyllo*-inositol dehydrogenase activity in the enzyme assay with the crude cell extract. Further work will be necessary to experimentally verify the periplasmic location of the *smc01163*-encoded dehydrogenase and to identify the substrate(s) and product(s) of the purified enzyme.

The inositol catabolism genes and their regulation are required for successful competition during alfalfa nodulation. The *idhA* mutants of *S. meliloti* and *R. leguminosarum* bv. *viciae* nodulated their host plants and fixed nitrogen at the same levels as the wild-type strains (14, 15, 29). Nevertheless, the *iolA* and *iolD* mutants of *R. leguminosarum* bv. *viciae* could not compete with the wild type in a competition assay (14). Our results showed that the *idhA*, *smc01163*, *iolA*, and the *iolRCDEB* mutants of *S. meliloti* nodulated alfalfa successfully when inoculated onto plants individually, but in cochallenge experiments the mutants were outcompeted by the wild type. This demonstrates that a functional inositol catabolism is required for *S. meliloti* to successfully compete during the process of host nodulation and colonization of nodules. It is worth emphasizing that the *iolR* mutant also could not compete against the wild type for nodule occupancy. The inositol catabolic genes are derepressed in the *iolR* mutant, which should allow an even higher rate of inositol catabolism. Thus, the correct regulation of inositol catabolism genes also appears to be required for *S. meliloti* to successfully compete for nodule occupancy, suggesting that the role of inositol isomers extends beyond being a nutrient source.

Recently, some inositol isomers have gained great interest in the medical field because of their therapeutic potentials (11, 21). Our study contributes a better understanding of inositol metabolism and emphasizes its role in symbiotic nitrogen fixation in agriculture. Since legume crops such as alfalfa plants contain inositol (9), the presence of inositol compounds may act as one of the signals for rhizobia in communicating the presence of potential host plants and may also sustain the rhizobia while they are moving toward the plant, during root hair attachment or multiplication in the infection thread or nodule. In fact, in soybean nodules induced by *Bradyrhizobium japonicum*, the second and third most abundant carbohydrates after sucrose are *myo*- and D-*chiro*-inositol, with 1 to 2 mg per g of nodule fresh weight (39). Also, inositol has been found to be exuded into soil by legume plants (45). Other inositol derivatives, the rhizopines *scyllo*-inosamine and L-3-*O*-methyl-*scyllo*-inosamine, have been termed nutritional mediators, because they represent exclusive carbon and nitrogen sources for the rhizobial strains that carry the rhizopine catabolism genes (26, 36, 38, 43). Rhizopine and inositol catabolism are interrelated, because a functional inositol catabolic pathway was shown to be required for the catabolism of rhizopines (2, 15, 38). Clearly, inositol compounds and the ability to catabolize them play important nutritional or signaling roles in the symbiotic relationship between rhizobia and legume plants.

ACKNOWLEDGMENTS

We thank an anonymous reviewer for improvements of the manuscript, Mariah Ramsdell and Lars Kohler for help with the preparation of 2-keto-*myo*-inositol, and Anke Becker and Michael Hynes for providing the *S. meliloti* 2011 mTn*5*-STM mutants and plasmid pJQ200SK, respectively.

This work was supported in part by a Dissertation Completion Fellowship and the Gwen Frostic Doctoral Fellowship from the Graduate College, by a Faculty Research and Creative Activities Award from Western Michigan University, and by the Herman Frasch Foundation.

REFERENCES

1. **Anderson, L.** 1972. The cyclitols, p. 519–579. *In* W. Pigman and D. Horton (ed.), The carbohydrates, 2nd ed., vol. 1A. Academic Press, New York, NY.
2. **Bahar, M., J. de Majnik, M. Wexler, J. Fry, P. S. Poole, and P. J. Murphy.** 1998. A model for the catabolism of rhizopine in *Rhizobium leguminosarum* involves a ferredoxin oxygenase complex and the inositol degradative pathway. Mol. Plant Microbe Interact. **11:**1057–1068.
3. **Beringer, J. E.** 1974. R factor transfer in *Rhizobium leguminosarum*. J. Gen. Microbiol. **84:**188–198.
4. **Berman, T., and B. Magasanik.** 1966. The pathway of *myo*-inositol degradation in *Aerobacter aerogenes*: dehydrogenation and dehydration. J. Biol. Chem. **241:**800–806.
5. **Boutte, C. C., B. S. Srinivasan, J. A. Flannick, A. F. Novak, A. T. Martens, S. Batzoglou, P. H. Viollier, and S. Crosson.** 2008. Genetic and computational identification of a conserved bacterial metabolic module. PLoS Genet. **4:**e1000310.
6. **Broughton, W. J., and M. J. Dilworth.** 1971. Control of leghaemoglobin synthesis in snake beans. Biochem. J. **125:**1075–1080.
7. **Carter, H. E., R. K. Clark, Jr., B. Lytle, and G. E. McCasland.** 1948. Oxidation of inositol by *Acetobacter suboxydans*. J. Biol. Chem. **174:**415–426.
8. **Daniellou, R., H. Zheng, D. M. Langill, D. A. Sanders, and D. R. Palmer.** 2007. Probing the promiscuous active site of *myo*-inositol dehydrogenase using synthetic substrates, homology modeling, and active site modification. Biochemistry **46:**7469–7477.
9. **Duke, J.** 1992. Handbook of phytochemical constituents of GRAS herbs and other economic plants. CRC Press, Inc., Boca Raton, FL.
10. **Egelhoff, T. T., and S. R. Long.** 1985. *Rhizobium meliloti* nodulation genes: identification of *nodDABC* gene products, purification of *nodA* protein and expression of *nodA* in *Rhizobium meliloti*. J. Bacteriol. **164:**591–599.
11. **Fenili, D., M. Brown, R. Rappaport, and J. McLaurin.** 2007. Properties of *scyllo*-inositol as a therapeutic treatment of AD-like pathology. J. Mol. Med. **85:**603–611.
12. **Figurski, D. H., and D. R. Helinski.** 1979. Replication of an origin-containing

derivative of plasmid RK2 dependent on a plasmid function provided *in trans*. Proc. Natl. Acad. Sci. U. S. A. **76:**1648–1652.
13. **Finan, T. M., B. Kunkel, G. F. De Vos, and E. R. Signer.** 1986. Second symbiotic megaplasmid in *Rhizobium meliloti* carrying exopolysaccharide and thiamine synthesis genes. J. Bacteriol. **167:**66–72.
14. **Fry, J., M. Wood, and P. S. Poole.** 2001. Investigation of *myo*-inositol catabolism in *Rhizobium leguminosarum* bv. *viciae* and its effect on nodulation competitiveness. Mol. Plant Microbe Interact. **14:**1016–1025.
15. **Galbraith, M. P., S. F. Feng, J. Borneman, E. W. Triplett, F. J. de Bruijn, and S. Rossbach.** 1998. A functional *myo*-inositol catabolism pathway is essential for rhizopine utilization by *Sinorhizobium meliloti*. Microbiology **144:**2915–2924.
16. **Jiang, G., A. H. Krishnan, Y. W. Kim, T. J. Wacek, and H. B. Krishnan.** 2001. A functional *myo*-inositol dehydrogenase gene is required for efficient nitrogen fixation and competitiveness of *Sinorhizobium fredii* USDA191 to nodulate soybean (*Glycine max* [L.] Merr.). J. Bacteriol. **183:**2595–2604.
17. **Kawsar, H. I., K. Ohtani, K. Okumura, H. Hayashi, and T. Shimizu.** 2004. Organization and transcriptional regulation of *myo*-inositol operon in *Clostridium perfringens*. FEMS Microbiol. Lett. **235:**289–295.
18. **Kiss, G. B., E. Vincze, Z. Kalman, T. Forrai, and A. Kondorosi.** 1979. Genetic and biochemical analysis of mutants affected in nitrate reduction in *Rhizobium meliloti*. J. Gen. Microbiol. **113:**105–118.
19. **Kroeger, C., and T. M. Fuchs.** 2009. Characterization of the *myo*-inositol utilization island of *Salmonella enterica* serovar Typhimurium. J. Bacteriol. **191:**545–554.
20. **Krol, E., and A. Becker.** 2004. Global transcriptional analysis of the phosphate starvation response in *Sinorhizobium meliloti* strains 1021 and 2011. Mol. Genet. Genomics **272:**1–17.
21. **Larner, J.** 2002. D-*chiro*-Inositol: its functional role in insulin action and its deficit in insulin resistance. Int. J. Exp. Diabetes Res. **3:**47–60.
22. **Loewus, F. A., and P. P. N. Murthy.** 2000. *myo*-Inositol metabolism in plants. Plant Sci. **150:**1–19.
23. **Meade, H. M., S. R. Long, G. B. Ruvkun, S. E. Brown, and F. M. Ausubel.** 1982. Physical and genetic characterization of symbiotic and auxotrophic mutants of *Rhizobium meliloti* induced by transposon Tn*5* mutagenesis. J. Bacteriol. **149:**114–122.
24. **Meade, H. M., and E. R. Signer.** 1977. Genetic mapping of *Rhizobium meliloti*. Proc. Natl. Acad. Sci. U. S. A. **74:**2076–2078.
25. **Morinaga, T., H. Ashida, and K. Yoshida.** 2010. Identification of two *scyllo*-inositol dehydrogenases in *Bacillus subtilis*. Microbiology **156:**1538–1546.
26. **Murphy, P. J., N. Heycke, Z. Banfalvi, M. E. Tate, F. J. de Bruijn, A. Kondorosi, J. Tempe, and J. Schell.** 1987. Genes for the catabolism and synthesis of an opine-like compound in *Rhizobium meliloti* are closely linked and on the Sym plasmid. Proc. Natl. Acad. Sci. U. S. A. **84:**493–497.
27. **Oke, V., and S. R. Long.** 1999. Bacterial genes induced within the nodule during the *Rhizobium*-legume symbiosis. Mol. Microbiol. **32:**837–849.
28. **Pobigaylo, N., D. Wetter, S. Szymczak, U. Schiller, S. Kurtz, F. Meyer, T. W. Nattkemper, and A. Becker.** 2006. Construction of a large signature-tagged mini-Tn*5* transposon library and its application to mutagenesis of *Sinorhizobium meliloti*. Appl. Environ. Microbiol. **72:**4329–4337.
29. **Poole, P. S., A. Blyth, C. J. Reid, and K. Walters.** 1994. *myo*-Inositol catabolism and catabolite regulation in *Rhizobium leguminosarum* bv. *viciae*. Microbiology **140:**2787–2795.
30. **Prentki, P., and H. M. Krisch.** 1984. *In vitro* insertional mutagenesis with a selectable DNA fragment. Gene **29:**303–313.
31. **Quandt, J., and M. F. Hynes.** 1993. Versatile suicide vectors which allow directed selection for gene replacement in Gram-negative bacteria. Gene **127:**15–21.
32. **Ramaley, R., Y. Fujita, and E. Freese.** 1979. Purification and properties of *Bacillus subtilis* inositol dehydrogenase. J. Biol. Chem. **254:**7684–7690.
33. **Rossbach, S., and F. J. de Bruijn.** 2007. Transposon mutagenesis, p. 684–708. *In* C. A. Reddy (ed.), Methods for general and molecular microbiology, 3rd ed. ASM, Washington, DC.
34. **Rossbach, S., D. A. Kulpa, U. Rossbach, and F. J. de Bruijn.** 1994. Molecular and genetic characterization of the (*mocABCR*) genes of *Rhizobium meliloti* L*5*-30. Mol. Gen. Genet. **245:**11–24.
35. **Rossbach, S., B. McSpadden, M. Ganoff, and F. J. de Bruijn.** 1995. *Rhizobium meliloti* rhizopine catabolism genes: distribution, role in competition and potential as marker gene to track microbes, p. 180–188. *In* M. Levin, C. Grim, and J. S. Angle (ed.), Biotechnology risk assessment. University of Maryland Biotechnology Institute, College Park, MD.
36. **Rossbach, S., G. Rasul, M. Schneider, B. Eardly, and F. J. de Bruijn.** 1995. Structural and functional conservation of the rhizopine catabolism (*moc*) locus is limited to selected *Rhizobium meliloti* strains and unrelated to their geographical origin. Mol. Plant Microbe Interact. **8:**549–559.
37. **Sambrook, J., E. F. Fritsch, and T. Maniatis.** 1989. Molecular cloning: a laboratory manual, 2nd ed. Cold Spring Harbor Laboratory Press, Cold Spring Harbor, NY.
38. **Schoffers, E., S. R. Gurung, P. R. Kohler, and S. Rossbach.** 2008. Chemical synthesis of *scyllo*-inosamine and catabolism studies in *Sinorhizobium meliloti*. Bioorg. Med. Chem. **16:**7838–7842.
39. **Streeter, J. G.** 1987. Carbohydrate, organic acid, and amino acid composition of bacteroids and cytosol from soybean nodules. Plant Physiol. **85:**768–773.
40. **Sundaram, T. K.** 1972. *myo*-Inositol catabolism in *Salmonella typhimurium*: enzyme repression dependent on growth history of organism. J. Gen. Microbiol. **73:**209–219.
41. **Turner, B. L., M. J. Paphazy, P. M. Haygarth, and I. D. McKelvie.** 2002. Inositol phosphates in the environment. Philos. Trans. R. Soc. Lond. B Biol. Sci. **357:**449–469.
42. **Wais, R. J., D. H. Wells, and S. R. Long.** 2002. Analysis of differences between *Sinorhizobium meliloti* 1021 and 2011 strains using the host calcium spiking response. Mol. Plant Microbe Interact. **15:**1245–1252.
43. **Wexler, M., D. M. Gordon, and P. J. Murphy.** 1995. The distribution of inositol rhizopine genes in *Rhizobium* populations. Soil Biol. Biochem. **27:**531–537.
44. **Wilson, K. J., S. G. Hughes, and R. A. Jefferson.** 1992. The *Escherichia coli gus* operon: introduction and expression of the *gus* operon in *E. coli* and the occurrence and use of GUS in other bacteria, p. 7–23. *In* S. R. Gallagher (ed.), GUS protocols: using the GUS gene as a reporter for gene expression. Academic Press, Inc., San Diego, CA.
45. **Wood, M., and A. P. Stanway.** 2001. *myo*-Inositol catabolism by *Rhizobium* in soil: HPLC and enzymatic studies. Soil Biol. Biochem. **33:**375–379.
46. **Yebra, M. J., M. Zuniga, S. Beaufils, G. Perez-Martinez, J. Deutscher, and V. Monedero.** 2007. Identification of a gene cluster enabling *Lactobacillus casei* BL23 to utilize *myo*-inositol. Appl. Environ. Microbiol. **73:**3850–3858.
47. **Yoshida, K., D. Aoyama, I. Ishio, T. Shibayama, and Y. Fujita.** 1997. Organization and transcription of the *myo*-inositol operon, *iol*, of *Bacillus subtilis*. J. Bacteriol. **179:**4591–4598.
48. **Yoshida, K., K. Kobayashi, Y. Miwa, C. M. Kang, M. Matsunaga, H. Yamaguchi, S. Tojo, M. Yamamoto, R. Nishi, N. Ogasawara, T. Nakayama, and Y. Fujita.** 2001. Combined transcriptome and proteome analysis as a powerful approach to study genes under glucose repression in *Bacillus subtilis*. Nucleic Acids Res. **29:**683–692.
49. **Yoshida, K., H. Sano, Y. Miwa, N. Ogasawara, and Y. Fujita.** 1994. Cloning and nucleotide sequencing of a 15 kb region of the *Bacillus subtilis* genome containing the *iol* operon. Microbiology **140:**2289–2298.
50. **Yoshida, K., M. Yamaguchi, T. Morinaga, M. Ikeuchi, M. Kinehara, and H. Ashida.** 2006. Genetic modification of *Bacillus subtilis* for production of D-*chiro*-inositol, an investigational drug candidate for treatment of type 2 diabetes and polycystic ovary syndrome. Appl. Environ. Microbiol. **72:**1310–1315.
51. **Yoshida, K., M. Yamaguchi, T. Morinaga, M. Kinehara, M. Ikeuchi, H. Ashida, and Y. Fujita.** 2008. *myo*-Inositol catabolism in *Bacillus subtilis*. J. Biol. Chem. **283:**10415–10424.